Dalton Transactions

Accepted Manuscript

ROYAL SOCIETY OF CHEMISTRY

www.rsc.org/dalton

Synthesis and reactivity of coordinatively unsaturated halocarbonyl molybdenum PNP pincer complexes

Sara R. M. M. de Aguiar,[a] Özgür Öztopcu,[a] Berthold Stöger,[b] Kurt Mereiter,[b] Luis F. Veiros,[c] Ernst Pittenauer,[b] Günter Allmaier,[b] and Karl Kirchner*,[a]

Abstract

In the present study a series of six-coordinate neutral 16e halocarbonyl Mo(II) complexes of the type [Mo(PNP^{Me}-*i*Pr)(CO)X_2] (X = I, Br, Cl), featuring the PNP pincer ligand N,N'-bis(diisopropylphosphino)-N,N'-dimethyl-2,6-diaminopyridine (PNP^{Me}-*i*Pr), were prepared and fully characterized. The synthesis of these complexes was accomplished by different methodologies depending on the halide ligands. For X = I and Br, [Mo(PNP^{Me}-*i*Pr)(CO)I_2] and [Mo(PNP^{Me}-*i*Pr)(CO)Br_2] were obtained by reacting [Mo(PNP^{Me}-*i*Pr)$(CO)_3$] with stoichiometric amounts of I_2 and Br_2, respectively. In the case of X = Cl, [Mo(PNP^{Me}-*i*Pr)(CO)Cl_2] was afforded by the reaction of $[Mo(CO)_4(\mu\text{-}Cl)Cl]_2$ with 1 equiv of PNP^{Me}-*i*Pr. The equivalent procedure also worked for X = Br. The modification of the 2,6-diaminopyridine scaffold by introducing NMe instead of NH spacers between the aromatic pyridine ring and the phosphine moieties changed the steric properties of the PNP-*i*Pr ligand significantly. While in the present case exclusively neutral six-coordinate complexes of the type [Mo(PNP^{Me}-*i*Pr)(CO)X_2] were obtained, with the parent PNP-*i*Pr ligand, i.e. featuring NH spacers, cationic seven-coordinate complexes of the type [Mo(PNP-*i*Pr)$(CO)_3$X]X were afforded. Upon treatment of [Mo(PNP^{Me}-*i*Pr)(CO)X_2] (X = Br, Cl) with Ag^+ in CH_3CN, the cationic complexes [Mo(PNP^{Me}-*i*Pr)(CO)$(CH_3CN)X]^+$ were formed. Halide abstraction from [Mo(PNP^{Me}-*i*Pr)(CO)Cl_2] in THF/CH_2Cl_2 afforded [Mo(PNP^{Me}-*i*Pr)(CO)(THF)Cl]$^+$. In keeping with the facile synthesis of monocationic complexes preliminary ESI-MS and DFT/B3LYP studies revealed that one halide ligand in complexes [Mo(PNP^{Me}-*i*Pr)(CO)X_2] is labile forming cationic fragments [Mo(PNP^{Me}-*i*Pr)(CO)X]$^+$ which react with molecular oxygen in parallel pathways to yield mono and dioxo Mo(IV) and Mo(VI) species. Structures of representative complexes were determined by X-ray single crystal analyses.

[a] Institute of Applied Synthetic Chemistry, Vienna University of Technology, Getreidemarkt 9, A-1060 Vienna, AUSTRIA, e-mail: kkirch@mail.tuwien.ac.at

[b] Institute of Chemical Technologies and Analytics, Vienna University of Technology, Getreidemarkt 9, A-1060 Vienna, AUSTRIA

[c] Centro de Química Estrutural, Instituto Superior Técnico, Universidade de Lisboa, Av. Rovisco Pais No. 1, 1049-001 Lisboa, PORTUGAL

†Electronic supplementary information (ESI) available. CCDC 1004519-1004523 for **3**, **4**, **5** and **8**. For ESI and crystallographic data in CIF or other electronic format see DOI: xxxxxxx.

Introduction

Tridentate PNP ligands in which a central pyridine-based ring donor contains -CH_2PR_2, OPR_2, or $NHPR_2$ substituents in the two *ortho* positions are widely utilized ligands in transition metal chemistry (e.g., Fe, Ru, Rh, Ir, Pd, Pt).[1,2,3] As group six PNP pincer complexes are concerned, only few examples have been described in the literature. Haupt and co-workers reported the synthesis of [M(PNP-Ph)$(CO)_3$] (M = Cr, Mo, W, PNP-Ph = N,N'-bis(diphenylphosphino)-N,N'-2,6-diaminopyridine),[4] while Walton and co-workers described the synthesis of the dinuclear molybdenum complex [Mo(PNP)Mo$(HPCy_2)Cl_3$] (PNP = 2,6-bis(dicyclohexylphosphinomethyl)pyridine).[5] Recently, dinuclear molybdenum and tungsten dinitrogen complexes bearing bulky PNP pincer ligands were found to work as effective catalysts for the formation of ammonia from dinitrogen.[6] The synthesis of a series of hydridocarbonyl and halocarbonyl tungsten pincer complexes featuring a related PNP pincer-type ligand based on silazane *viz* $HN(SiMe_2CH_2PPh_2)_2$ were described by Templeton and coworkers.[7]

We are currently focusing on the synthesis and reactivity of molybdenum complexes containing PNP pincer ligands based on the 2,6-diaminopyridine scaffold. In these ligands the aromatic pyridine ring and the phosphine moieties are connected via NH, N-alkyl, or N-aryl spacers. The latter have a profound impact on the sterics of the ligands and consequently also on the reactivity of transition metal PNP complexes. This was shown recently in the course of the synthesis of a series of Mo(II) PNP halocarbonyl complexes of the types $[Mo(PNP)(CO)_3X]^+$ (X = I, Br, Cl) (**I**) and $[Mo(PNP)(CO)_2X_2]$ (X = I, Br, Cl, F) (**II**) as illustrated in Chart 1.[8,9,10] Complexes based on the parent PNP ligands bearing NH moieties form cationic hepta-coordinated monohalo species with three CO ligands (complexes **I**) with both PPh_2 and P*i*Pr_2 moieties, whereas the PNP ligands bearing NMe moieties lead to formation of neutral dihalo species that are either hepta-coordinate and feature two CO ligands (with PPh_2 substituents, complexes **II**) or hexa-coordinate and feature only one CO ligand (with P*i*Pr_2 substituents, complexes **III**). On the other hand, the formation of the hydridocarbonyl complexes of the type $[Mo(PNP)(CO)_3H]^+$ (X = I, Br, Cl) was independent of the nature of the amine linker.[10]

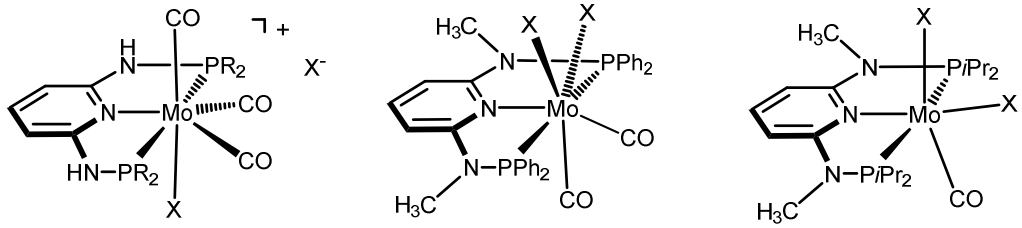

Chart 1 Halocarbonyl Mo(II) PNP pincer complexes as a function of the PR_2 moieties and the NR spacers

In continuation of our studies on molybdenum PNP complexes, we report here on the synthesis, characterization, and reactivity of a series of coordinatively unsaturated halocarbonyl molybdenum(II) PNP pincer complexes of the type $[Mo(PNP^{Me}\text{-}iPr)(CO)X_2]$ (X = I, Br, Cl) (**III**) where the P*i*Pr_2 moieties of the PNP ligand are connected to the pyridine ring via NMe spacers. Moreover, evidence for the formation of mono

and dioxo molybdenum complexes is provided based on ESI-MS measurements and supported by DFT calculations. X-ray structures of representative complexes will be given.

Results and Discussion

Treatment of **2** with stoichiometric amounts of X_2 (X = I, Br) in CH_2Cl_2 yields the neutral six-coordinate complexes [Mo(PNP^{Me}-*i*Pr)(CO)I_2] (**3**) and [Mo(PNP^{Me}-*i*Pr)(CO)Br_2] (**4**) in 90 and 95% isolated yield (Scheme 1). With Cl_2 gas, no clean reaction took place presumably due to overoxidation and formation of several paramagnetic intractable materials. However, the analogous chlorine complex [Mo(PNP^{Me}-*i*Pr)(CO)Cl_2] (**5**) was afforded by treatment of [Mo(CO)$_4$(μ-Cl)Cl]$_2$ with 1 equiv of PNP^{Me}-*i*Pr (**1**) in CH_2Cl_2 in 92% isolated yield. The latter methodology is also a convenient alternative route to obtain **4**.

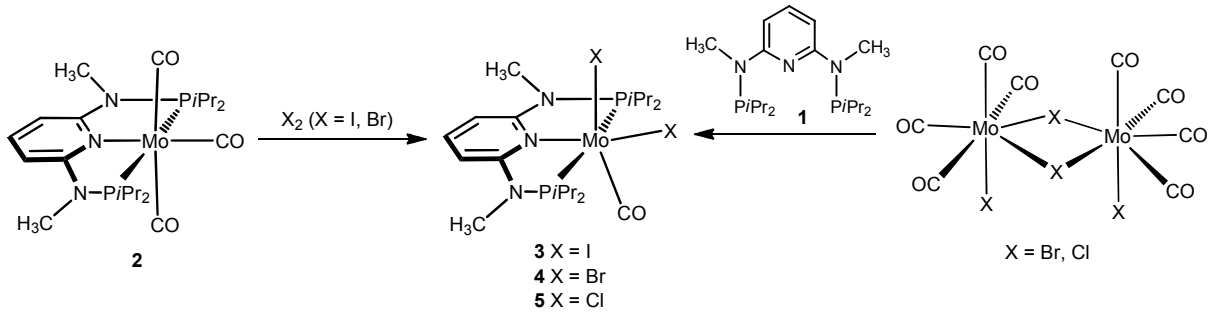

Scheme 1. Synthesis of halocarbonyl Mo(II) PNP pincer complexes of the type [Mo(PNP^{Me}-*i*Pr)(CO)X_2] (X = I, Br, Cl)

Attempts to obtain the analogous fluorine complex [Mo(PNP^{Me}-*i*Pr)(CO)F_2] upon addition of 1 equiv of 1-fluoro-2,4,6-trimethylpyridinium as the tetrafluoroborate salt, which is known to act as net source of "F^+" while the BF_4^- counterion donates fluoride ions,[7,9] to a solution of [Mo(PNP^{Me}-*i*Pr)(CO)$_3$] in CH_2Cl_2 was unsuccessful. It is interesting to note that there was no evidence for the formation of the cationic complexes [Mo(PNP^{Me}-*i*Pr)(CO)$_3$X]$^+$ (**A**) as in the case of the PNP-*i*Pr ligand.

Despite of their low formal electron count, all complexes are thermally robust bluish-green solids which are air stable in the solid state. In solution they decompose slowly within a few days. Characterization was accomplished by a combination of elemental analysis and by ^{1}H, ^{13}C{^{1}H} and ^{31}P{^{1}H} NMR, and IR spectroscopy. The ^{13}C{^{1}H} NMR spectrum of **3**-**5** give rise to characteristic low-field triplet resonances at 247.3, 247.9, and 248.5 ppm, respectively, with coupling constants $^2J_{PC}$ in the range of 26.5 -35.2 Hz assignable to the carbon atoms of the CO ligand. In the ^{31}P{^{1}H} NMR spectrum singlets at 190.4, 195.2, and 197.9 ppm, respectively, are observed. The chemical shifts are in line with the increasing electronegativity of the halide ligands. In the IR spectrum complexes **3**-**5** exhibit one strong ν_{CO} band at 1824, 1816, and 1813 cm^{-1}, respectively (*cf* 2143 cm^{-1} in free CO) which suggests that Cl^- is a better electron donor. For comparison, complexes [Mo(PNP^{Me}-Ph)(CO)$_2$X$_2$] (X = I, Br, Cl, F) (**B**) give rise to two strong CO stretching vibrations in the range of 2000 to 1858 cm^{-1} due to weaker π-back-bonding interactions and thus the metal

center in [Mo(PNP^{Me}-*i*Pr)(CO)X_2] seems to be slightly more electron rich than in the seven coordinate complexes [Mo(PNP^{Me}-Ph)$(CO)_2X_2$].

In addition to the NMR and IR spectroscopic characterization, the solid state structures of **3**, **4**, and **5** were determined by single-crystal X-ray diffraction. Structural diagrams are depicted in Figures 1 - 3 with selected bond distances given in the captions. Molybdenum is coordinated by the tridentate PNP ligand in a meridional fashion. The one carbonyl and the two halide ligands define a second meridional arrangement so that the coordination geometry around the molybdenum center corresponds to a distorted octahedron with the atom pairs P1/P2 N1/X1, and C20/X2. Except for the Mo-halide bond lengths, the bond distances and bond angles and conformations of the three complexes **3**, **4**, and **5**, are very similar and average to Mo-C 1.919 Å, Mo-N 2.270 Å, and Mo-P 2.374 Å. Compared with [Mo(PNP^{Me}-*i*Pr)$(CO)_3$] (**2**), which adopts mm2 symmetry with Mo, P, N, pyridine and one CO perfectly coplanar, complexes **3**-**5** possess a characteristic common distortion by which molybdenum is located about 0.5 Å above and the two P atoms by 0.4 Å below the reference plane of the pyridine ring. While Mo-N and Mo-P bonds in **2** and **3**-**5** are similar, this deformation leads to a decrease in the intramolecular P-P distance from 4.7 in **2** to 4.25 Å in **3**-**5** and of the P-Mo-P angle from ca. 155° in **2** to 126-128° in **3**-**5**. This means that the PNP ligand in **3**-**5** is on a transition from meridional to facial coordination that would end with a final ideal P-Mo-P angle of 90°. By a concomitant rotation of the P*i*Pr_2 fragments about their N-P bonds the space between the *i*Pr_2 fragments on the upper side of the complex above Mo (C6, C7, C8 and C12, C13, C14) becomes more open, while below (C9, C10, C10 and C15, C16, C17) it becomes more congested (Figure 2). A distortion of the Mo coordination figure similar to **3**-**5** has been previously observed for the seven-coordinate complexes [Mo(PNP^{Me}-Ph)$(CO)_2X_2$] (X = Cl, Br, I) in which the *i*Pr_2 fragment is replaced by the less bulky PPh_2 fragment and the two halogen atoms are in *cis*-disposition and oriented approximately parallel to the P1-P2 vector instead perpendicular to it like in **3**-**5**.[9]

Figures 1 -3 (hereabouts)

The electronic structure of complex **4** was evaluated by DFT calculations. In the frontier orbitals calculated for complex **4**, one can observe the splitting of the metal *d* orbitals that is expected in a distorted octahedral d^4 complex. As expected, all orbitals represented in Figure 4 have an important contribution from Mo *d* orbitals. There is a lower energy group of three orbitals that would correspond to the t_{2g} set in a perfect octahedral molecule, and then the two *d* orbitals pointing directly to the coordinated atoms that would correspond to the $2e_g$ set in a symmetric molecule. In the "t_{2g}" set the first two orbitals are occupied, being HOMO-1 and HOMO, and show a Mo–Br π^* character indicating that the bromine ligands are acting as π-donors compensating the electron deficiency of the molybdenum center. This is reflected in a significant participation of the Br ligands on the electron density of those orbitals (see Figure 4). In the "$2e_g$" set, the x^2-y^2 orbital lies in an equatorial plane defined by the three coordinating atoms of the PNP ligand and by the Br ligand *trans* to pyridine N-atom, while the z^2 orbital points towards the two axial ligands, the Br-atom and the CO ligand *trans* to each other.

Figure 4

Treating [Mo(PNP^{Me}-*i*Pr)(CO)(Br)$_2$] (**4**) and [Mo(PNP^{Me}-*i*Pr)(CO)(Cl)$_2$] (**5**) with $AgSbF_6$ in the coordinating solvent CH_3CN led to the immediate precipitation of AgCl and subsequent formation of the bluish-green cationic 16e complexes [Mo(PNP^{Me}-*i*Pr)(CO)(CH_3CN)(Br)]$^+$ (**6**) and [Mo(PNP^{Me}-*i*Pr)(CO)(CH_3CN)(Cl)]$^+$ (**7**), respectively, which could be isolated in pure form in 90% yield (Scheme 2). Surprisingly, the same reaction with [Mo(PNP^{Me}-*i*Pr)(CO)(I)$_2$] (**3**) did not afford this type of complex but an as yet not identified new major species exhibiting a $^{31}P\{^1H\}$ NMR resonance at 148 ppm. Complexes **6** and **7** are thermally stable both in the solid state and in solution if air is excluded but readily decompose in the presence of oxygen to give several as yet not identified (oxidation) products. The sensitivity towards oxygen in comparison to complexes **3**-**5** may be due to the lability of these complexes which are actually latent 14e systems. Characterization of **6** and **7** was accomplished by elemental analysis and by ^1H, $^{13}C\{^1H\}$ and $^{31}P\{^1H\}$ NMR, and IR spectroscopy. The $^{13}C\{^1H\}$ NMR spectrum of **6** and **7** exhibit the characteristic low-field resonances of the CO ligand as poorly-resolved broad signals at 230.1 and 235.0 ppm, respectively. In the $^{31}P\{^1H\}$ NMR spectrum of these complexes singlets at 179.4 and 186.0 ppm were observed. Due to the decreased electron donor strengths of the molybdenum center, in the cationic complexes **6** and **7** the CO stretching frequencies are shifted to higher wavenumbers (1840 and 1836 cm^{-1}) as compared to those of the neutral compounds **3**-**5**.

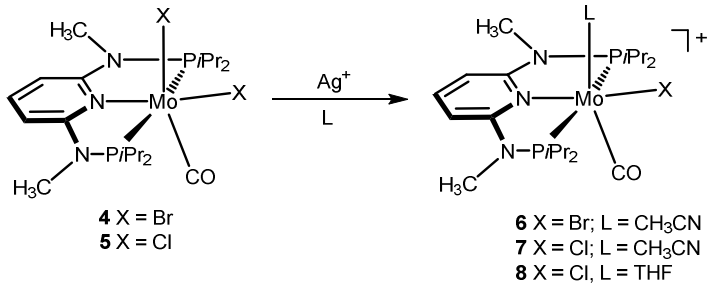

4 X = Br
5 X = Cl

6 X = Br; L = CH_3CN
7 X = Cl; L = CH_3CN
8 X = Cl, L = THF

Scheme 2 Synthesis of cationic complexes [Mo(PNP^{Me}-*i*Pr)(CO)(L)(X)]$^+$ (X = Br, Cl; L = CH_3CN, THF) upon halide abstraction with Ag^+.

Attempts to crystallize either **6** and **7** from CH_3CN solutions for an X-ray diffraction analysis gave large and highly solvated but very unstable crystals for which only a poor crystal structure model could be derived that showed the coordinated acetonitrile molecule in *trans* disposition to CO.[11] However, from a THF solution of **7** as the SbF_6^- salt crystals of [Mo(PNP^{Me}-*i*Pr)(CO)(THF)Cl]SbF_6 (**8**) were obtained where the CH_3CN ligand was replaced by a THF molecule. Complex **8** could be obtained directly by treating of **5** with 1 equiv of $AgSbF_6$ in a mixture of CH_2Cl_2/THF (9:1). A structural view of **8** is depicted in Figure 5 with selected bond distances given in the caption. This complex features essentially the same coordination geometry about Mo like the dihalogenide precursors **3**, **4**, and **5**. Thus, in **8** all bond distances involving Mo except for the Mo-O_{THF} agree within 0.02 Å with those of **5**, and also bond angles, the distance P1-P2, and other geometric parameters are in good agreement with **3**, **4**, and **5**.

Figure 5

ESI-MS enables not only the detection and the study of reaction substrates and products but also short-lived reaction intermediates and decomposition products as they are present in solution. Accordingly, solutions of **3-5** in CH_3CN and the corresponding sodium halide were subjected to ESI-MS analysis in the positive ion mode. Under so called "soft ionization" conditions, in the absence of air signals corresponding to the sodiated complexes [Mo(PNP^{Me}-*i*Pr)(CO)X_2] ([M+Na]$^+$) and also [Mo(PNP^{Me}-*i*Pr)(CO)X]$^+$ (**A**, [M-X]$^+$) where one halide ligand is dissociated. The formation of **A** is in keeping with the fact that the halide *trans* to the CO ligand is labile. In the presence of air additional species could be detected which no longer feature a CO ligand, but contain both one oxygen atom [Mo(PNP^{Me}-*i*Pr)(O)X]$^+$ ([M–X-CO+O]$^+$ (**B**) and two oxygen atoms [Mo(PNP^{Me}-*i*Pr)$(O)_2$X]$^+$ ([M–X-CO+2O]$^+$ (**C** or **D**). Moreover, for X = I and Br a different dioxo species with the general formula [Mo(PNP^{Me}-*i*Pr)$(O)_2$]$^+$ (M-2X+2O]$^+$ (**E**) was detected, presumably due to loss of an iodine and bromine radical, respectively. It interesting to mention that in the case of [Mo(PNP^{Me}-*i*Pr)$(CO)I_2$] (**3**) all dioxygen containing fragments as well as **A** vanished after 24 h to yield among several intractable species the doubly oxidized both protonated and sodiated PNP^{Me}-*i*Pr ligand (m/z 402.2 and 424.2), while the signal of the mono oxo species **B** remained. Positive ion ESI full scan mass spectra of **3** and **4** are depicted in Figures 6 and 7. Possible structures based on their m/z values are shown in Scheme 3.

Figures 6 and **7**

The stability of [M–X-CO+2O]$^+$ (**C** or **D**) was further tested in CID (MS/MS) experiments revealing that no O_2 release took place. This observation seems to support the formation of a *cis* dioxo Mo(VI) complex (**D**). rather than a molybdenum species with a κ^2-bound O_2 ligand (**C**). This is also supported by DFT calculations utilizing the cationic complex [Mo(PNP^{Me}-*i*Pr)(CO)Br]$^+$ (**A**) as model system. The optimized structures and the free energy balances for the reaction steps are depicted in Figure 8. The highly unsaturated 14e species [Mo(PNP^{Me}-*i*Pr)(CO)Br]$^+$ is almost equally stable in the triplet state, ^{3}**A**, and in the singlet state, ^{1}**A** (ΔG = 1.8 kcal/mol). Addition of oxygen to any of those species would lead to the cationic mono oxo Mo(IV) complex [Mo(PNPMe-*i*Pr)(O)(Br)]$^+$ (**B**) or to the dioxygen Mo(IV) and Mo(VI) species [Mo(PNPMe-*i*Pr)(κ^2-O_2)(Br)]$^+$ (**C**) or *cis*-[Mo(PNPMe-*i*Pr)$(O)_2$(Br)]$^+$ (^{1}**D**), respectively. Complex **C** is slightly more stable in the triplet state (^{3}**C**), while the opposite is observed for the mono oxo species, where ^{1}**B** is significantly more stable than ^{3}**B** (by 18.5 kcal/mol). All O_2 addition steps are thermodynamically strongly favored (see Figure 7). ^{1}**B** and ^{1}**D** are the most stable products for each O-stoichiometry, the corresponding reactions being exergonic by 59.9 and 85.9 kcal/mol, respectively. Also, given the stability differences, the κ^2-O_2 species **C** are probably intermediates in the formation of ^{1}**D** as the dioxo product. Accordingly, based on the ESI-MS measurements and the DFT calculations we believe that the predominant ^{1}**B** and ^{1}**D** are formed if complexes [Mo(PNPMe-*i*Pr)$(CO)X_2$] are exposed to air. It has to be noted that a related mono oxo Mo(IV) PCP pincer complex was recently formed as side product while synthesizing a Mo(IV) PCP nitride complex.[12] Molybdenum complexes with the *cis*-$[MoO_2]^{2+}$ core, on the other hand, are very common which have found wide applications in organic synthesis due to their oxidation properties.[13]

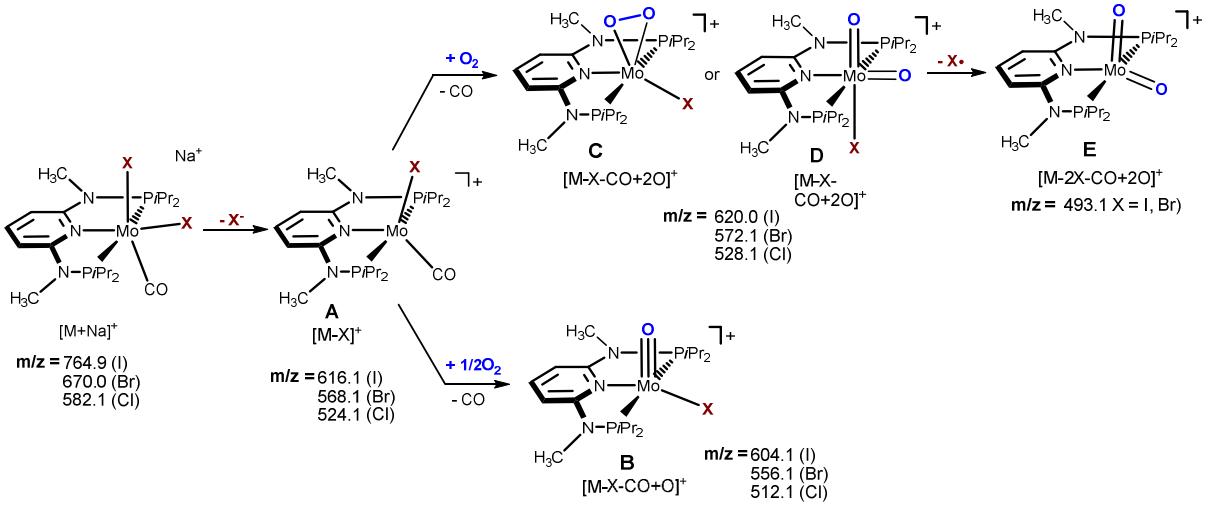

Scheme 3 Fragmentation pathways of [Mo(PNP^{Me}-*i*Pr)(CO)X_2] (**3**-**5**) in CH_3CN in the presence of molecular oxygen as established by ESI MS experiments. Structural suggestions are based on DFT calculations.

Conclusion

In the present study we prepared a series of six-coordinate neutral 16e halocarbonyl Mo(II) complexes of the type [Mo(PNP^{Me}-*i*Pr)(CO)X_2] (X = I, Br, Cl) featuring the PNP pincer ligand N,N'-bis(diisopropylphosphino)-N,N'-dimethyl-2,6-diaminopyridine (PNP^{Me}-*i*Pr). The modification of the 2,6-diaminopyridine scaffold by introducing NMe instead of NH spacers between the aromatic pyridine ring and the phosphine moieties changed the steric properties of the PNP-*i*Pr ligand significantly. While in the present case exclusively neutral six-coordinate 16e complexes of the type [Mo(PNP^{Me}-*i*Pr)(CO)X_2] were obtained, with the parent PNP-*i*Pr ligand, i.e. featuring NH spacers, cationic seven-coordinate 18e complexes of the type [Mo(PNP-*i*Pr)$(CO)_3X]^+$ were afforded. These complexes react in the presence of Ag^+ in coordinating solvents such as CH_3CN and THF to give the cationic complexes [Mo(PNP^{Me}-*i*Pr)(CO)$(CH_3CN)X]^+$ (X = Br, Cl) and [Mo(PNP^{Me}-*i*Pr)(CO)$(THF)Cl]^+$ were the CH_3CN and THF ligands are coordinated *trans* to the CO ligand. In keeping with the facile synthesis of mono cationic complexes, preliminary ESI MS studies and DFT/B3LYP calculations support that one halide ligand in [Mo(PNP^{Me}-*i*Pr)(CO)X_2] is labile to give the cationic formally 14e fragments [Mo(PNP^{Me}-*i*Pr)(CO)$X]^+$ which are able to react with molecular oxygen in parallel pathways to yield mono and dioxo Mo(IV) and Mo(VI) species. A detailed experimental and theoretical study in order to establish the nature of these oxygen containing molybdenum species and the mechanisms of the corresponding reactions are currently underway and results will be reported in due course.

Experimental Section

General. All manipulations were performed under an inert atmosphere of argon by using Schlenk techniques. The solvents were purified according to standard procedures.[14] The ligand and complexes N,N'-bis(diisopropylphosphino)-N,N'-dimethyl-2,6-diaminopyridine (PNP^{Me}-*i*Pr) (**1**), $[Mo(CO)_4(\mu\text{-}X)X]_2$ (X = Cl, Br), and [Mo(PNP^{Me}-*i*Pr)$(CO)_3$] (**2**) were prepared according to the literature.[10] The deuterated solvents were

purchased from Aldrich and dried over 4 Å molecular sieves. ^{1}H, $^{13}C\{^{1}H\}$, and $^{31}P\{^{1}H\}$ NMR spectra were recorded on Bruker AVANCE-250, AVANCE-300 DPX, and AVANCE-400 spectrometers. ^{1}H and $^{13}C\{^{1}H\}$ NMR spectra were referenced internally to residual protio-solvent, and solvent resonances, respectively, and are reported relative to tetramethylsilane (δ = 0 ppm). $^{31}P\{^{1}H\}$ NMR spectra were referenced externally to H_3PO_4 (85%) (δ = 0 ppm).

All mass spectrometric measurements were performed on an Esquire 3000^{plus} 3D-quadrupole ion trap mass spectrometer (Bruker Daltonics, Bremen, Germany) in positive-ion mode electrospray ionization (ESI-MS). Mass calibration was done with a commercial mixture of perfluorinated trialkyl-triazines (ES Tuning Mix, Agilent Technologies, Santa Clara, CA, USA). All analytes were dissolved in CH_3CN "Lichrosolv" quality (Merck, Darmstadt, Germany) to a concentration of roughly 1 mg/mL and doped with sodium halides (Merck, Darmstadt, Germany) to avoid or suppress dissociation of halogen substituents from the molybdenum complexes as previously described for molybdenum complexes.[9] Direct infusion experiments were carried out using a Cole Parmer model 74900 syringe pump (Cole Parmer Instruments, Vernon Hills, IL, USA) at a flow rate of 2 μl/min. Full scan and MS/MS-scans were measured in the range m/z 100-1000 with the target mass set to m/z 800. Further experimental conditions include: drying gas temperature: 150°C; capillary voltage: -4 kV; skimmer voltage: 40 V; octapole and lens voltages: according to the target mass set. Helium was used as buffer gas for full scans and as collision gas for MS/MS-scans in the low energy CID (collision induced dissociation) mode. The activation and fragmentation width for tandem mass spectrometric (MS/MS) experiments was set to 10 - 12 Da to cover the entire isotope cluster for fragmentation. The corresponding fragmentation amplitude ranged from 0.3 to 0.8 V in order to keep a low abundant precursor ion intensity in the resulting MS/MS spectrum. As precursor ions for tandem mass spectrometric experiments the ions $[M+Na]^+$, $[M-X]^+$, $[M-X-CO+O]^+$ and $[M-X-CO+2O]^+$ could be selected as precursor ions. All mass calculations are based on the lowest mass molybdenum isotope (^{92}Mo-isotope). Mass spectra and tandem spectra were averaged during data acquisition time of 1 to 2 min and one analytical scan consisted of five successive micro scans resulting in 50 and 100 analytical scans, respectively, for the final mass spectrum or MS/MS spectrum.

[Mo(PNP^{Me}-*i*Pr)(CO)I$_2$] (3). A solution of [Mo(PNP^{Me}-*i*Pr)(CO)$_3$] (**2**) (100 mg, 0.180 mmol) in CH_2Cl_2 (10 mL) was treated with I_2 (49 mg, 0.190 mmol) and the solution was stirred for 4 h at room temperature. The solution was then filtered through Celite. After removal of the solvent under reduced pressure, a blue-green solid was obtained which was washed twice with diethyl ether (10 mL) and dried under vacuum. Yield: 121 mg (90%). Anal. Calcd for $C_{20}H_{37}I_2MoN_3OP_2$ (747.23): C, 32.15; H, 4.99; N, 5.62. Found: C, 32.19; H, 5.09; N, 5.58. ^{1}H NMR (δ, $CDCl_3$, 20 ^{o}C): 7.66 (t, J = 8.3 Hz, 1H, py), 6.22 (d, J = 8.3 Hz, 2H, py), 3.13 (s, 6H, NCH_3), 2.78 (m, 2H, $CH(CH_3)_2$), 2.37 (m, 2H, $CH(CH_3)_2$), 1.39 (m, 18H, $CH(CH_3)_2$), 0.72 (d, J = 6.9 Hz, 3H, $CH(CH_3)_2$), 0.66 (d, J = 6.9 Hz, 3H, $CH(CH_3)_2$). $^{13}C\{^{1}H\}$ NMR (δ, CD_2Cl_2, 20 ^{o}C): 247.3 (t, J = 26.5 Hz, CO), 162.0 (t, J = 7.6 Hz, py), 142.3 (s, py), 99.1 (s, py), 34.4 (t, J = 2.7 Hz, $N(CH_3)_2$), 30.2 (d, J = 28.8 Hz, $CH(CH_3)_2$), 20.0 (d, J = 18.3 Hz, $CH(CH_3)_2$), 19.2 (s, $CH(CH_3)_2$), 17.8 (s, $CH(CH_3)_2$), 17.7 (s, $CH(CH_3)_2$), 16.9 (s, $CH(CH_3)_2$). $^{31}P\{^{1}H\}$ NMR (δ, $CDCl_3$, 20 ^{o}C): 190.4. IR (ATR, cm^{-1}): 1824 (ν_{co}). ESI-MS (*m/z,* CH_3CN, NaI) positive ion: 764.9 $[M+Na]^+$, 616.1 $[M-I]^+$. In the presence of air: 604.1 $[M-I-CO+O]^+$, 620.0 $[M-I-CO+2O]^+$, 493.1 $[M-2I-CO+2O]^+$.

[Mo(PNP^{Me}-*i*Pr)(CO)Br$_2$] (4). This complex was prepared analogously to **3a** with **2** (100 mg, 0.180 mmol) and Br_2 (0.10 µL, 0.19 mmol) as starting materials. Yield: 113 mg (95%). Anal. Calcd for $C_{20}H_{37}Br_2MoN_3OP_2$ (653.23): C, 36.77; H, 5.71; N, 6.43. Found: C, 36.65; H, 5.59; N, 6.42. C, 36.77; H, 5.71; N, 6.43. ^{1}H NMR (δ, $CDCl_3$, 20 °C): 7.58 (t, *J* = 8.3 Hz, 1H, py), 6.21 (d, *J* = 8.0 Hz, 2H, py), 3.14 (s, 6H, NC*H*$_3$), 2.81 (m, 2H, C*H*(CH$_3$)$_2$), 2.56 (m, 2H, C*H*(CH$_3$)$_2$), 1.52 (d, *J* = 6.9 Hz, 3H, CH(C*H*$_3$)$_2$), 1.45 (d, *J* = 6.8 Hz, 3H, CH(C*H*$_3$)$_2$), 1.29 (m, 12H, CH(C*H*$_3$)$_2$), 0.71 (d, *J* = 7.0 Hz, 3H, CH(C*H*$_3$)$_2$), 0.64 (d, *J* = 7.0 Hz, 3H, CH(C*H*$_3$)$_2$). ^{13}C{^{1}H} NMR (δ, $CDCl_3$, 20 °C): 247.9 (t, *J* = 32.0 Hz, *C*O), 161.5 (t, *J* = 8.1 Hz, py), 141.0 (s, py), 98.2 (s, py), 34.6 (s, N(*C*H$_3$)$_2$), 30.2 (d, *J* = 29.1 Hz, *C*H(CH$_3$)$_2$), 20.3 (d, *J* = 24.5 Hz, *C*H(CH$_3$)$_2$), 18.2 (s, CH(*C*H$_3$)$_2$), 17.9 (s, CH(*C*H$_3$)$_2$), 17.5 (s, CH(*C*H$_3$)$_2$), 16.3 (s, CH(*C*H$_3$)$_2$). ^{31}P{^{1}H} NMR (δ, $CDCl_3$, 20 °C): 195.2. IR (ATR, cm^{-1}): 1816 (ν_{co}). ESI-MS (*m/z,* CH_3CN, NaBr) positive ion: 670.0 [M+Na]$^+$, 568.1 [M-Br]$^+$. In the presence of air: 556.1 [M-Br-CO+O]$^+$, 572.1 [M-Br-CO+2O]$^+$, 493.1 [M-2Br-CO+2O]$^+$.

[Mo(PNP^{Me}-*i*Pr)(CO)Cl$_2$] (5). A solution of [Mo(CO)$_4$(µ-Cl)Cl]$_2$ (150 mg, 0.27 mmol) in CH_2Cl_2 (10 mL) was treated with 1 equiv. of **1** (209 mg, 0.56 mmol) and the solution was stirred for 4 h at room temperature. The solution was then filtered through Celite. After removal of the solvent under reduced pressure, a blue-green solid was obtained which was washed twice with diethyl ether (10 mL) and dried under vacuum. Yield: 140 mg (92%). Anal. Calcd for $C_{20}H_{37}Cl_2MoN_3OP_2$ (564.33): C, 42.57; H, 6.61; N, 7.45. Found: C, 42.65; H, 6.51; N, 7.55. ^{1}H NMR (δ, $CDCl_3$, 20 °C): 7.58 (t, *J* = 8.8 Hz, 1H, py), 6.19 (d, *J* = 7.8 Hz, 2H, py), 3.14 (s, 6H, NC*H*$_3$), 2.82 (m, 2H, C*H*(CH$_3$)$_2$), 2.69 (m, 2H, C*H*(CH$_3$)$_2$), 1.51 (d, *J* = 6.3 Hz, 3H, CH(C*H*$_3$)$_2$), 1.44 (d, *J* = 6.3 Hz, 3H, CH(C*H*$_3$)$_2$), 1.30 (m, 12H, CH(C*H*$_3$)$_2$), 0.71 (d, *J* = 6.7 Hz, 3H, CH(C*H*$_3$)$_2$), 0.65 (d, *J* = 6.7 Hz, 3H, CH(C*H*$_3$)$_2$). ^{13}C{^{1}H} NMR (δ, CD_2Cl_2, 20 °C): 248.5 (t, *J* = 35.2 Hz, *C*O), 161.3 (t, *J* = 7.1 Hz, py), 140.8 (s, py), 97.9 (s, py), 34.4 (s, N(*C*H$_3$)$_2$), 30.2 (d, *J* = 29.93 Hz, *C*H(CH$_3$)$_2$), 21.3 (d, *J* = 26.3 Hz, *C*H(CH$_3$)$_2$), 17.8 (s, CH(*C*H$_3$)$_2$), 17.6 (s, CH(*C*H$_3$)$_2$), 17.4 (s, CH(*C*H$_3$)$_2$), 16.0 (s, CH(*C*H$_3$)$_2$). ^{31}P{^{1}H} NMR (δ, $CDCl_3$, 20 °C): 197.9. IR (ATR, cm^{-1}): 1813 (ν_{co}). ESI-MS (*m/z,* CH_3CN, NaCl) positive ion: 582.1 [M+Na]$^+$, 524.1 [M-Cl]$^+$. In the presence of air: 512.1 [M-Cl-CO+O]$^+$, 528.1 [M-Cl-CO+2O]$^+$.

[Mo(PNP^{Me}-*i*Pr)(CO)(CH$_3$CN)Br]SbF$_6$ (6). A solution of [Mo(PNP^{Me}-*i*Pr)(CO)(Br)$_2$] (**4**) (300 mg, 0.46 mmol) in CH_3CN (10 mL) was reacted with $AgSbF_6$ (165 mg, 0.48 mmol) and the mixture was stirred for 16h. After filtration over glass wool and Celite, the solvent was removed under reduced pressure and a blue-green solid was obtained which was washed twice with diethyl ether (10 mL) and dried under vacuum. Yield: 390 mg (90%). Anal. Calcd for $C_{22}H_{40}BrF_6MoN_4OP_2Sb$ (850.12): C, 31.08; H, 4.74; N, 6.59. Found: C, 31.12; H, 4.81; N, 6.62. ^{1}H NMR (δ, CD_2Cl_2, 20 °C): 7.65 (t, *J* = 8.0 Hz, 1H, py), 6.40 (d, *J* = 7.5 Hz, 2H, py), 3.12 (s, 6H, NC*H*$_3$), 2.80 (m, 2H, C*H*(CH$_3$)$_2$), 2.67 (m, 2H, C*H*(CH$_3$)$_2$), 2.20 (s, 3H, NCC*H*$_3$), 1.28 (m, 12H, CH(C*H*$_3$)$_2$), 1,07 (m, 12H, CH(C*H*$_3$)$_2$). ^{13}C{^{1}H} NMR (δ, CD_2Cl_2, 20 °C): 230.1 (*C*O), 162.1 (t, *J* = 6.4 Hz, py), 143.6 (s, py), 132.4 (s, N*C*CH$_3$), 99.0 (s, py), 34.6 (s, N(*C*H$_3$)$_2$), 30.7 (d, *J* = 27.0 Hz, *C*H(CH$_3$)$_2$), 22.1 (d, *J* = 20.1 Hz, *C*H(CH$_3$)$_2$), 17.5 (s, CH(*C*H$_3$)$_2$), 17.2 (s, CH(*C*H$_3$)$_2$), 17.3 (s, CH(*C*H$_3$)$_2$), 15.7 (s, NC*C*H$_3$). ^{31}P{^{1}H} NMR (δ, CD_2Cl_2, 20 °C): 179.4. IR (ATR, cm^{-1}): 2279 ($\nu_{C\equiv N}$), 1840 (ν_{co}). ESI-MS (*m/z,* CH_3CN) positive ion: 568.1 [M-Br]$^+$.

[Mo(PNP^{Me}-*i*Pr)(CO)(CH$_3$CN)Cl]SbF$_6$ (7). This complex was prepared analogously to **6** with **5** (150 mg, 0.26 mmol) and $AgSbF_6$ (95 mg, 0.28 mmol) as starting materials. Yield: 195 mg (90%). Anal. Calcd for $C_{22}H_{40}ClF_6MoN_4OP_2Sb$ (806.67): C, 32.80; H, 5.00; N, 6.95. Found: C, 32.85; H, 4.89; N, 7.02. ^{1}H NMR (δ,

$CDCl_3$, 20 °C): 7.79 (t, *J* = 8.1 Hz, 1H, py), 6.48 (d, *J* = 8.1 Hz, 2H, py), 3.65 (s, 6H, NCH_3), 3.26 (m, 2H, CH(CH_3)$_2$), 2.85 (m, 2H, CH(CH_3)$_2$), 2.23 (s, 3H, NCCH_3), 1.41 (m, 12H, CH(CH_3)$_2$), 1,15 (m, 12H, CH(CH_3)$_2$).$^{13}C\{^1H\}$ NMR (δ, CD_2Cl_2, 20 °C): 235.0 (*C*O), 162.0 (t, *J* = 7.8 Hz, py), 143.7 (s, py), 130.0 (s, N*C*CH_3), 99.8 (s, py), 35.2 (s, N(*C*H_3)$_2$), 30.7 (d, *J* = 23.6 Hz, *C*H(CH_3)$_2$), 22.5 (d, *J* = 28.8 Hz, *C*H(CH_3)$_2$), 18.0 (s, CH(*C*H_3)$_2$), 17.9 (s, CH(*C*H_3)$_2$), 17.7 (s, CH(*C*H_3)$_2$), 16.1 (s, CH(*C*H_3)$_2$), 15.5 (s, NC*C*H_3). $^{31}P\{^1H\}$ NMR (δ, CD_2Cl_2, 20 °C): 186.0. IR (ATR, cm^{-1}): 2277 ($\nu_{C\equiv N}$), 1836 (ν_{co}). ESI-MS (*m/z,* CH_3CN) positive ion: 582.1 $[M\text{-}Cl]^+$.

[Mo(PNP^{Me}-*i*Pr)(CO)(THF)Cl]SbF$_6$ (8). A solution of [Mo(PNP^{Me}-*i*Pr)(CO)$(Cl)_2$] (**5**) (150 mg, 0.26 mmol) in a mixture of CH_2Cl_2/THF (9:1) (10 mL) was reacted with $AgSbF_6$ (95 mg, 0.28 mmol) and the mixture was stirred for 16h. After filtration over glass wool and Celite, the solvent was removed under reduced pressure and a blue-green solid was obtained which was washed twice with diethyl ether (10 mL) and dried under vacuum. Yield: 195 mg (90%). Anal. Calcd for $C_{24}H_{45}ClF_6MoN_3O_2P_2Sb$ (836.72): C, 34.45; H, 5.42; N, 5.02. Found: C, 34.35; H, 5.39; N, 5.10. ^1H NMR (δ, CD_2Cl_2, 20 °C): 7.83 (t, *J* = 7.4 Hz, 1H, py), 6.43 (d, *J* = 7.1 Hz, 2H, py), 3.71 (m, 4H, THF), 3.23 (s, 6H, NCH_3), 2.85 (m, 4H, CH(CH_3)$_2$), 1.85 (m, 4H, THF), 1.38 (m, 18H, CH(CH_3)$_2$), 1,14 (m, 6H, CH(CH_3)$_2$) $^{13}C\{^1H\}$ NMR (δ, CD_2Cl_2, 20 °C): 218.5 (*C*O), 162.3 (t, *J* = 6.8 Hz, py), 146.0 (s, py), 128.9 (s, py), 74.4 (s, THF), 36.3 (s, N(*C*H_3)$_2$), 31.0 (t, *J* = 12.45 Hz, *C*H(CH_3)$_2$), 25.5 (s, THF), 19.5 (s, CH(*C*H_3)$_2$), 19.2 (s, CH(*C*H_3)$_2$), 19.0 (s, CH(*C*H_3)$_2$), 18.8 (s, CH(*C*H_3)$_2$). $^{31}P\{^1H\}$ NMR (δ, CD_2Cl_2, 20 °C): 193.9. IR (ATR, cm^{-1}): 1831 (ν_{co}).

X-ray Structure Determination. Single crystals of the complexes **3**, **4**, **5**, and **8** suitable for X-ray diffraction were obtained by the solvent/antisolvent liquid-vapour diffusion method at room temperature using CH_2Cl_2/pentane (**3, 4, 5**) or THF/diethyl ether (**8**). X-ray diffraction data were collected at *T* = 100K on a Bruker Kappa APEX-2 CCD area detector diffractometer using graphite-monochromated Mo-Kα radiation (*λ* = 0.71073 Å) and *φ*- and *ω*-scan frames covering complete spheres of the reciprocal space with θ_{max} = 30°. Corrections for absorption and *λ*/2 effects were applied using program SADABS.[15] After structure solution with program SHELXS97 refinement on F^2 was carried out with program SHELXL97.[16] Non-hydrogen atoms were refined anisotropically. Hydrogen atoms were placed in calculated positions and thereafter treated as riding. Crystal data are reported in Table 1, detailed structural data are given in CIF format in the Supporting information. Variata: Complexes **4** (Br) and **5** (Cl) are isostructural, but not **3** (I) which contains two instead of one independent Mo complex in the asymmetric unit**.** These two independent complexes in **3** are similar in bond lengths and bond angles, except that the first of the two is ordered while the second one has two isopropyl groups orientation disordered. The crystal structures of **4** (Br) and **5** (Cl) exhibit larger unoccupied voids of ca. 50 $Å^3$ in their lattices. Interestingly, it was found that the Br complex **4** can crystallize in a second crystal form (polymorph) which has a more efficient packing and no significant voids in the lattice. Crystal data for this form are given in the ESI (CCDC 1004523).

Computational Details All calculations were performed using the GAUSSIAN 09 software package[17] on the Phoenix Linux Cluster of the Vienna University of Technology. The optimized geometries were obtained with the B3LYP functional,[18] without symmetry constraints. That functional includes a mixture of Hartree-Fock[19] exchange with DFT[20] exchange-correlation, given by Becke's three parameter functional with the Lee, Yang and Parr correlation functional, which includes both local and non-local terms. The basis set

used for the geometry optimizations consisted of the Stuttgart/Dresden ECP (SDD) basis set[21] to describe the electrons of molybdenum, and a standard 6-31g** basis set[22] for all other atoms. Frequency calculations were performed confirming all optimized structures as minima (zero imaginary frequency modes). The free energy values presented where obtained at 298.15 K and 1 atm by using zero point energy and thermal energy corrections based on structural and vibration frequency data. Three-dimensional representations of the orbitals were obtained with Molekel.[23]

Acknowledgement. Financial support by the Austrian Science Fund (FWF) (Project No. P24202-N17) and by Fundação para a Ciência e Tecnologia, FCT (PEst-OE/QUI/UI0100/2013) is gratefully acknowledged. The ESI mass spectrometer was made available by Austrian Science Fund (FWF) (Project No. P15008-N03 to GA). The X-ray center of the Vienna University of Technology is acknowledged for financial support and for providing access to the single-crystal diffractometer.

Table 1. Details for the crystal structure determinations of compounds [Mo(PNP^{Me}-*i*Pr)(CO)I_2] (**3**), [Mo(PNP^{Me}-*i*Pr)(CO)Br_2] (**4**), [Mo(PNP^{Me}-*i*Pr)(CO)Cl_2] (**5**), and [Mo(PNP^{Me}-*i*Pr)(CO)(THF)Cl]SbF_6 (**8**).

.

	3	**4**	**5**	**8**
formula	$C_{20}H_{37}I_2MoN_3OP_2$	$C_{20}H_{37}Br_2MoN_3OP_2$	$C_{20}H_{37}Cl_2MoN_3OP_2$	$C_{24}H_{45}ClF_6MoN_3O_2P_2Sb$
fw	747.21	653.23	564.31	836.71
cryst.size, mm	0.30 x 0.20 x 0.02	0.28 x 0.25 x 0.23	0.48 x 0.44 x 0.25	0.28 x 0.22 x 0.18
color, shape	green plate	green block	green block	green block
crystal system	monoclinic	monoclinic	monoclinic	monoclinic
space group	$P2_1/c$ (no. 14)	$P2_1/n$ (no. 14)	$P2_1/n$ (no. 14)	$P2_1/c$ (no. 14)
a, Å	20.8211(7)	15.3996(8)	15.2750(3)	11.4932(4)
b, Å	15.7605(5)	11.2076(5)	11.3110(2)	9.6174(3)
c, Å	17.6677(6)	15.6189(7)	15.3045(3)	29.2482(10)
α, deg	90	90	90	90
β, deg	114.312(2)	105.005(2)	106.401(1)	92.387(2)
γ, deg	90	90	90	90
V, Å^3	5283.5(3)	2603.8(2)	2536.65(8)	3230.14(19)
T, K	100(2)	100(2)	100(2)	100(2)
Z	8, (*Z'* = 2)	4	4	4
ρ_{calc}, g cm^{-3}	1.879	1.666	1.478	1.721
μ, mm^{-1} (MoKα)	2.971	3.712	0.871	1.468
F(000)	2912	1312	1168	1680
absorption corrections	multi-scan, 0.94-0.47	multi-scan, 0.44-0.36	multi-scan, 0.75-0.70	multi-scan, 0.77-0.65
θ range, deg	2.15–30.00	2.16–30.00	2.22–30.00	2.21–30.00
no. of rflns measd	86452	54727	39490	80030
R_{int}	0.050	0.023	0.018	0.026
no. of rflns unique	15409	7581	7384	9421
no. of rflns $I>2\sigma(I)$	12721	7003	7091	8736
no. of params / restraints	564 / 0	272 / 0	272 / 0	383 / 0
R_1 ($I > 2\sigma(I)$) [a]	0.0265	0.0195	0.0169	0.0437
R_1 (all data)	0.0392	0.0229	0.0178	0.0476
wR_2 ($I > 2\sigma(I)$)	0.0510	0.0483	0.0447	0.0998
wR_2 (all data)	0.0553	0.0498	0.0453	0.1027
Diff.Four.peaks min/max, eÅ^{-3}	-0.82 / 1.22	-0.38 / 1.15	-0.36 / 0.84	-1.52 / 1.48

[a] $R1 = \Sigma||F_o|-|F_c|| / \Sigma|F_o|$, $wR2 = \{\Sigma[w(F_o^2 - F_c^2)^2] / \Sigma[w(F_o^2)^2]\}^{½}$, GooF = $\{\Sigma[w(F_o^2 - F_c^2)^2] / (n-p)\}^{½}$

References

1 For reviews on pincer complexes, see: (a) M. Albrecht and G. Van Koten, *Angew. Chem., Int. Ed.* 2001, **40**, 3750. (b) M. E. Van der Boom and D. Milstein, *Chem. Rev.* 2003, **103**, 1759. (c) J. T. Singleton, *Tetrahedron* 2003, **59**, 1837. (d) P. Bhattacharya and H. Guan, *Comment Inorg. Chem.* 2011, **32**, 88. (e) S. Schneider, J. Meiners and B. Askevold, *Eur. J. Inorg. Chem.* 2012, 412. (f) D. Morales-Morales and C. M. Jensen, Eds. The Chemistry of Pincer Compounds; Elsevier: Amsterdam, 2007. (g) D. Benito-Garagorri and K. Kirchner, *Acc. Chem. Res.* 2008, **41**, 201.

2 For recent stoichiometric reactions involving PNP pincer complexes, see: (a) M. Vogt, M. Gargir, M. A. Iron, Y. Diskin-Posner, Y. Ben-David and D. Milstein, *Chem. Eur. J.* 2012, **18**, 9194. (b) M. Vogt, O. Rivada-Wheelaghan, M. A. Iron, G. Leitus, Y. Diskin-Posner, L. J. W. Shimon, Y. Ben-David and D. Milstein, *Organometallics* 2013, **32**, 300. (c) M. Montag, J. Zhang and D. Milstein, *J. Am. Chem. Soc.* 2012, **134**, 10325. (d) M. Feller, Y. Diskin-Posner, L. J. W. Shimon, E. Ben-Ari and D. Milstein, *Organometallics* 2012, **31**, 4083.

3 For recent catalytic reactions involving PNP pincer complexes, see: (a) E. Balaraman, E. Khaskin, G. Leitus and D. Milstein, *Nature Chemistry* 2013, **5**, 122. (b) D. Srimani, M. Feller, Y. Ben-David and D. Milstein, *Chem. Commun.* 2012, **48**, 11853. (c) D. Srimani, E. Balaraman, B. Gnanaprakasam, Y. Ben-David and D. Milstein, *Adv. Synth. Catal.* 2012, **354**, 2403. (d) E. Kossoy, Y. Diskin-Posner, G. Leitus and D. Milstein, *Adv. Synth. Catal.* 2012, **354**, 497. (e) L. Schwartsburd, M. A. Iron, L. Konstantinowski, E. Ben-Ari and D. Milstein, *Organometallics* 2011, **30**, 2721.

4 (a) W. Schirmer, U. Flörke and H. J. Haupt, Z. Anorg. Allg. Chem. 1987, **545**, 83; (b) W. Schirmer, U. Flörke and H. J. Haupt, *Z. Anorg. Allg. Chem.* 1989, **574**, 239.

5 (a) H.-F. Lang, P. E. Fanwick and R. A. Walton, *Inorg. Chim. Acta* 2002, **329**, 1.

6 (a) K. Arashiba, S. Kuriyama, K. Nakajima and Y. Nishibayashi, *Chem. Commun.* 2013, **49**, 11215. (b) E. Kinoshita, K. Arashiba, S. Kuriyama, Y. Miyake, R. Shimazaki, H. Nakanishi and Y. Nishibayashi, *Organometallics* 2012, **31**, 8437. (c) A. Arashiba, K. Sasaki, S. Kuriyama, Y. Miyake, H.; Nakanishi and Y. Nishibayashi, *Organometallics* 2012, **31**, 2035. (d) K. Arashiba, Y. Miyake and Y. Nishibayashi, Y. *Nat. Chemistry,* 2011, **3**, 120.

7 L. A. Wingard, P. S. White and J. L. Templeton. *Dalton Trans*., **2012**, 41, 11438.

8 D. Benito-Garagorri, E. Becker, J. Wiedermann, W. Lackner, M. Pollak, K. Mereiter, J. Kisala and K. Kirchner, *Organometallics* 2006, **25**, 1900.

9 S. R. M. M. de Aguiar, B. Stöger, E. Pittenauer, G. Allmaier, M. Puchberger, L. F. Veiros and K. Kirchner, *J. Organomet. Chem.* 2014, **760**, 74.

10 Ö. Öztopcu, C. Holzhacker, M. Puchberger, M. Weil, K. Mereiter, L. F. Veiros and K. Kirchner, *Organometallics* 2013, **32**, 3042.

11 A structural diagram of complex **6** according to X-ray analysis is given in the ESI, but a CIF of this structure was not deposited due to its insufficient quality.

12 T. J. Hebden, R. R. Schrock, M. K. Takase and P. Müller, *Chem. Commun.* 2012, **48**, 1851.

13 F. E. Kühn, A. M. Santos and M. Abrantes *Chem. Rev.* 2006, **106**, 2455

14 D. D. Perrin and W. L. F. Armarego, Purification of Laboratory Chemicals, 3rd ed.; Pergamon: New York, 1988.

15 Bruker programs: APEX2, version 2009.9–0; SAINT, version 7.68 A; SADABS, version 2008/1; SHELXTL, version 2008/4, Bruker AXS Inc., Madison, WI, 2009.

16 G. M. Sheldrick, *Acta Cryst.* 2008, **A64**, 112.

17 Gaussian 09, Revision A.02, M. J. Frisch, G. W. Trucks, H. B. Schlegel, G. E. Scuseria, M. A. Robb, J. R. Cheeseman, G. Scalmani, V. Barone, B. Mennucci, G. A. Petersson, H. Nakatsuji, M. Caricato, X. Li, H. P. Hratchian, A. F. Izmaylov, J. Bloino, G. Zheng, J. L. Sonnenberg, M. Hada, M. Ehara, K. Toyota, R. Fukuda, J. Hasegawa, M. Ishida, T. Nakajima, Y. Honda, O. Kitao, H. Nakai, T. Vreven, J. A. Montgomery, Jr., J. E. Peralta, F. Ogliaro, M. Bearpark, J. J. Heyd, E. Brothers, K. N. Kudin, V. N. Staroverov, R. Kobayashi, J. Normand, K. Raghavachari, A. Rendell, J. C. Burant, S. S. Iyengar, J. Tomasi, M. Cossi, N. Rega, J. M. Millam, M. Klene, J. E. Knox, J. B. Cross, V. Bakken, C. Adamo, J. Jaramillo, R. Gomperts, R. E. Stratmann, O. Yazyev, A. J. Austin, R. Cammi, C. Pomelli, J. W. Ochterski, R. L. Martin, K. Morokuma, V. G. Zakrzewski, G. A. Voth, P. Salvador, J. J. Dannenberg, S. Dapprich, A. D. Daniels, Ö. Farkas, J. B. Foresman, J. V. Ortiz, J. Cioslowski, and D. J. Fox, Gaussian, Inc., Wallingford CT, 2009.

18 (a) A. D. Becke, *J. Chem. Phys.* 1993, **98**, 5648. (b) B. Miehlich, A. Savin, H. Stoll and H. Preuss, *Chem. Phys. Lett* 1989, **157**, 200. (c) C. Lee, W. Yang and G. Parr, *Phys. Rev. B* 1988, **37**, 785.

19 W. J. Hehre, L. Radom, P. v. R. Schleyer and J. A. Pople, *Ab Initio Molecular Orbital Theory*. John Wiley & Sons, New York, 1986.

20 R. G. Parr & W. Yang, in Density Functional Theory of Atoms and Molecules; Oxford University Press: New York, 1989.

21 (a) U. Haeusermann, M. Dolg, H. Stoll and H. Preuss, *Mol. Phys.* 1993, **78**, 1211; (b) W. Kuechle, M. Dolg, H. Stoll and H. Preuss, *J. Chem. Phys.* 1994, **100**, 7535; (c) T. Leininger, A. Nicklass, H. Stoll, M. Dolg and P. Schwerdtfeger, *J. Chem. Phys.* 1996, **105**, 1052.

22 (a) A. D. McLean and G. S. Chandler, *J. Chem. Phys.* 1980, **72**, 5639; (b) R. Krishnan, J. S. Binkley, R. Seeger and J. A. Pople, *J. Chem. Phys.* 1980, **72**, 650; (c) P. J. Hay, *J. Chem. Phys.* 1977, **66**, 4377; (d) K. Raghavachari and G. W. Trucks, *J. Chem. Phys.* 1989, **91**, 1062; (e) R. C. Binning and L. A. Curtiss, *J. Comput. Chem.* 1995, *10*3, 6104; (f) M. P. McGrath and L. Radom, *J. Chem. Phys.* 1991, **94**, 511.

23 S. Portmann and H. P. Lüthi, *Chimia,* 2000, **54**, 766.

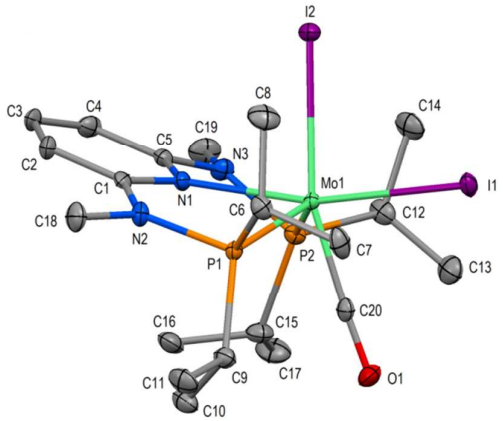

Figure 1. Structural view of [Mo(PNP^{Me}-*i*Pr)(CO)I_2] (**3**) showing 50% thermal ellipsoids (H atoms and a second independent complex omitted for clarity). Selected bond lengths (Å) and bond angles (°): Mo-N(1) 2.275(2), Mo-C(20) 1.915(3), Mo-P(1) 2.3825(7), Mo-P(2) 2.3764(7), Mo-I(1) 2.7657(3), Mo-I(2) 2.8504(3); P(1)-Mo-P(2) 126.11(2), N(1)-Mo-P(1) 74.11(6), N(1)-Mo-P(2) 70.91(6), N(1)-Mo-I(1) 165.50(5), N(1)-Mo-I(2) 79.54(5), N(1)-Mo-C(20) 115.13(9), I(1)-Mo-I(2) 86.36(1), I(1)-Mo-C(20) 79.32(8), I(2)-Mo-C(20) 163.17(7).

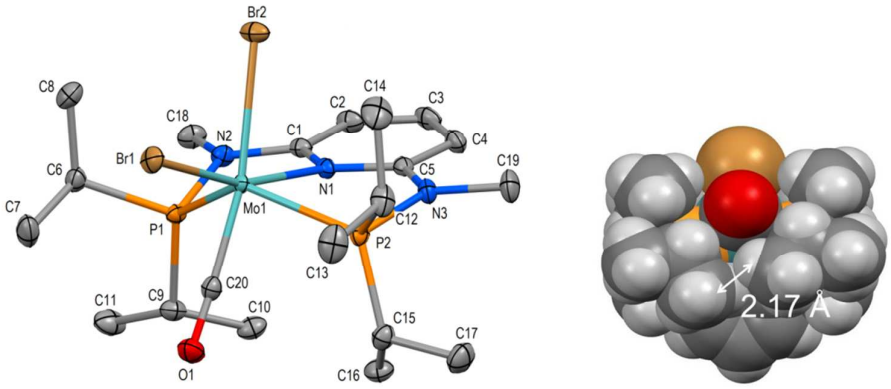

(a) **(b)**

Figure 2. (**a**) Structural view of [Mo(PNP^{Me}-*i*Pr)(CO)Br_2] (**4**) showing 50% thermal ellipsoids (H atoms omitted for clarity). Selected bond lengths (Å) and bond angles (°): Mo-N(1) 2.2665(12), Mo-C(20) 1.9209(15), Mo-P(1) 2.3847(4), Mo-P(2) 2.3620(4), Mo-Br(1) 2.5494(2), Mo-Br(2) 2.6301(3); P(1)-Mo-P(2) 128.01(2), N(1)-Mo-P(1) 72.13(3), N(1)-Mo-P(2) 73.97(3), N(1)-Mo-Br(1) 163.60(3), N(1)-Mo-Br(2) 78.98(3), N(1)-Mo-C(20) 115.05(5), Br(1)-Mo-Br(2) 84.79(1), Br(1)-Mo-C(20) 81.26(4), Br(2)-Mo-C(20) 165.88(4). (b) Space filling representation including H atoms to illustrate crowding. Viewed down the O1-C20-Mo1-Br2 axis revealing a relatively close contact between *i*Pr moieties of the PNP^{Me}-*i*Pr ligand.

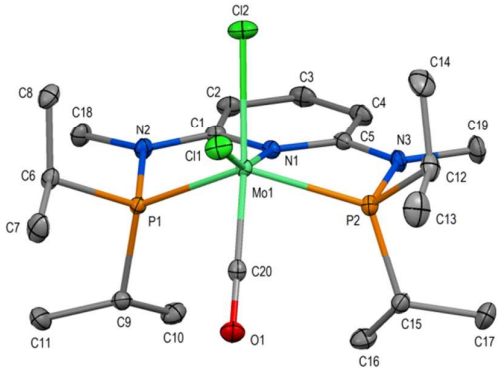

Figure 3. Structural view of [Mo(PNP^{Me}-*i*Pr)(CO)Cl$_2$] (**5**) showing 50% thermal ellipsoids (H atoms omitted for clarity). Selected bond lengths (Å) and bond angles (°): Mo-N(1) 2.2691(8), Mo-C(20) 1.9208(10), Mo-P(1) 2.3783(3), Mo-P(2) 2.3579(3), Mo-Cl(1) 2.4052(2), Mo-Cl(2) 2.4792(3); P(1)-Mo-P(2) 128.03(1), N(1)-Mo-P(1) 72.20(2), N(1)-Mo-P(2) 73.65(2), N(1)-Mo-Cl(1) 163.04(2), N(1)-Mo-Cl(2) 79.27(2), N(1)-Mo-C(20) 114.82(4), Cl(1)-Mo-Cl(2) 83.88(1), Cl(1)-Mo-C(20) 82.07(3), Cl(2)-Mo-C(20) 165.87(3).

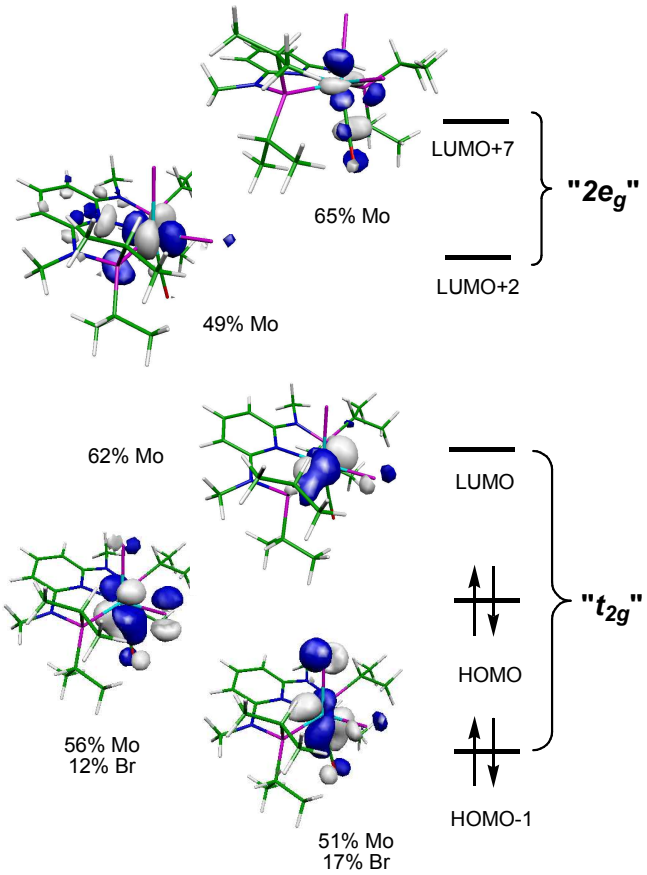

Figure 4. Frontier orbitals (*d* splitting) of [Mo(PNP^{Me}-*i*Pr)(CO)Br$_2$] (**4**).

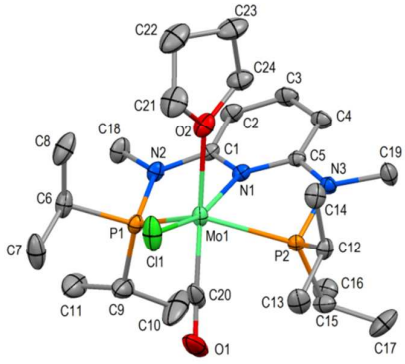

Figure 5. Structural view of [Mo(PNP^{Me}-*i*Pr)(CO)(THF)Cl]SbF_6 (**8**) showing 50% thermal ellipsoids (H atoms and SbF_6^- anion omitted for clarity). Selected bond lengths (Å) and bond angles (°): Mo-N(1) 2.260(2), Mo-C(20) 1.913(4), Mo-P(1) 2.3853(9), Mo-P(2) 2.3717(8), Mo-Cl(1) 2.3966(8), Mo-O(2) 2.312(3); P(1)-Mo-P(2) 125.66(4), N(1)-Mo-P(1) 73.80(6), N(1)-Mo-P(2) 71.82(6), N(1)-Mo-Cl(1) 162.97(9), N(1)-Mo-O(2) 80.18(9), N(1)-Mo-C(20) 113.20(14), Cl(1)-Mo-O(2) 83.09(7), Cl(1)-Mo-C(20) 83.79(13), O(2)-Mo-C(20) 165.21(13).

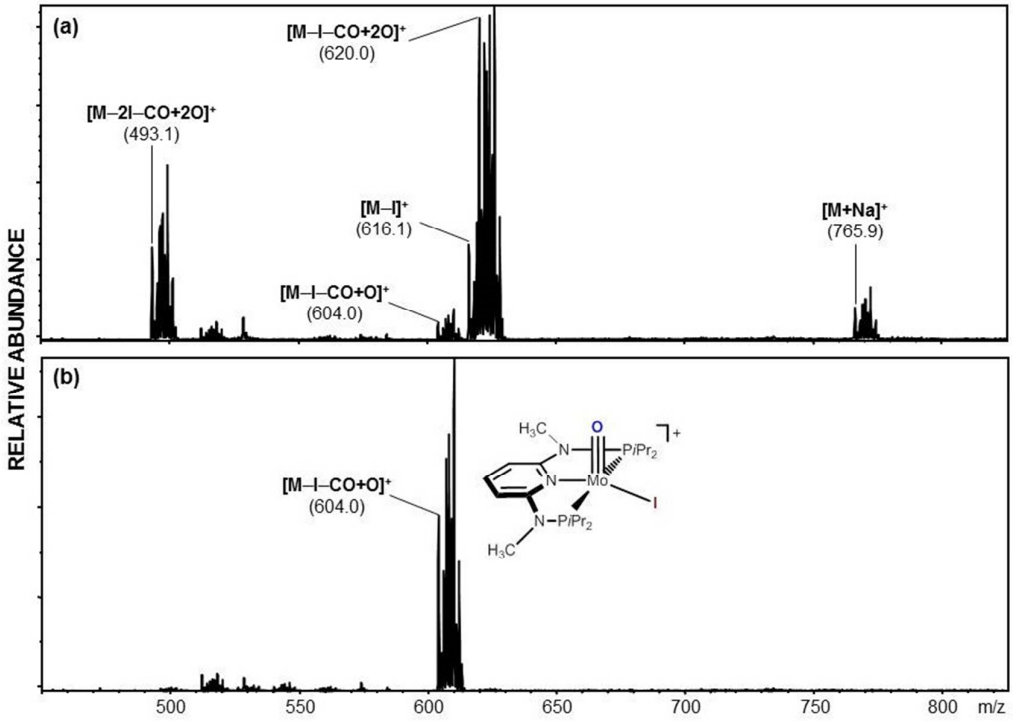

Figure 6. Positive-ion full scan ESI-MS of [Mo(PNP^{Me}-*i*Pr)(CO)I_2] (**3**) in CH_3CN in the presence of air after 15 min (a) and after 24 h (b).

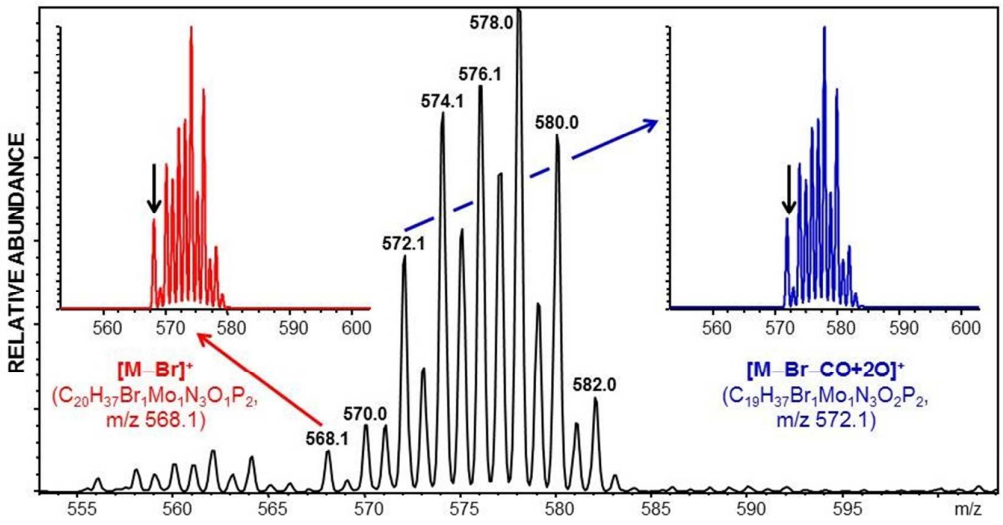

Figure 7 Positive-ion ESI-MS of [Mo(PNP^{Me}-*i*Pr)(CO)Br$_2$] (**4**) in CH_3CN covering the mass region of the [M-Br]$^+$ and the [M-Br-CO+2O]$^+$ fragments. Insets show the isotope pattern match for [Mo(PNP^{Me}-*i*Pr)(CO)Br]$^+$ ([M-Br]$^+$) and [Mo(PNP^{Me}-*i*Pr)(O)$_2$Br]$^+$ ([M-Br-CO+2O]$^+$)

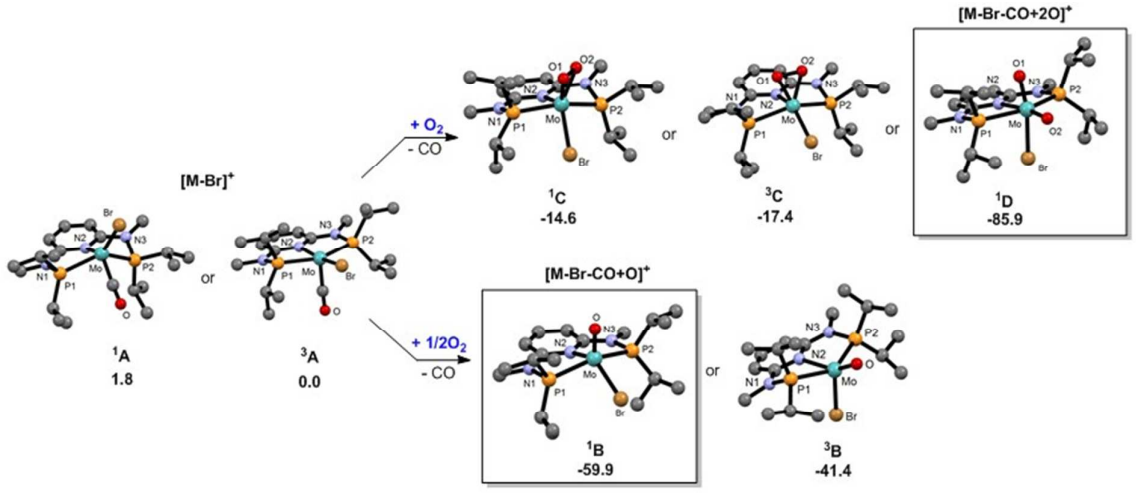

Figure 8 Reactions of [Mo(PNP^{Me}-*i*Pr)(CO)Br]$^+$ (**A**) in the presence of air based on ESI-MS experiments and DFT/B3LYP calculations (free energies in kcal/mol).

TOC

A series of six-coordinate neutral 16e halocarbonyl Mo(II) complexes of the type [Mo(PNP^{Me}-*i*Pr)(CO)X_2] (X = I, Br, Cl) were prepared and fully characterized. These complexes feature PNP ligands based on the 2,6-diaminopyridine scaffold with NMe spacers between the pyridine ring and the phosphine moieties.